UC Riverside

UC Riverside Previously Published Works

Title

Digitonin-facilitated delivery of imaging probes enables single-cell analysis of AKT signalling activities in suspension cells

Permalink

https://escholarship.org/uc/item/8wc9p9sz

Journal

Analyst, 146(17)

ISSN

0003-2654

Authors

Wang, Siwen
Perkins, Nicole G
Ji, Fei
et al.

Publication Date

2021-09-07

DOI

10.1039/d1an00751c

Peer reviewed

eScholarship.org Powered by the California Digital Library
University of California

Author Manuscript

Author Manuscript

Author Manuscript

Author Manuscript

HHS Public Access

Author manuscript

Analyst. Author manuscript; available in PMC 2022 September 07.

Published in final edited form as:

Analyst. 2021 September 07; 146(17): 5307–5315. doi:10.1039/d1an00751c.

Digitonin-facilitated delivery of imaging probes enables single-cell analysis of AKT signalling activities in suspension cells

Siwen Wang[a], **Nicole G. Perkins**[a], **Fei Ji**[a], **Rohit Chaudhuri**[a], **Zhili Guo**[a], **Priyanka Sarkar**[a], **Shiqun Shao**[a], **Zhonghan Li**[a], **Min Xue**[a]

[a]Department of Chemistry, University of California, Riverside, Riverside, California 92521, United States.

Abstract

Analyzing intracellular signalling protein activities in living cells promises a better understanding of the signalling cascade and related biological processes. We have previously developed cyclic peptide-based probes for analyzing intracellular AKT signalling activities, but these peptide probes were not cell-permeable. Implementing fusogenic liposomes as delivery vehicles could circumvent the problem when analyzing adherent cells, but it remained challenging to study suspension cells using similar approaches. Here, we present a method for delivering these imaging probes into suspension cells using digitonin, which could transiently perforate the cell membrane. Using U87, THP-1, and Jurkat cells as model systems representing suspended adherent cells, myeloid cells, and lymphoid cells, we demonstrated that low concentrations of digitonin enabled a sufficient amount of probes to enter the cytosol without affecting cell viability. We further combined this delivery method with a microwell single-cell chip and interrogated the AKT signalling dynamics in THP-1 and Jurkat cells, followed by immunofluorescence-based quantitation of AKT expression levels. We resolved the cellular heterogeneity in AKT signalling activities and showed that the kinetic patterns of AKT signalling and the AKT expression levels were related in THP-1 cells, but decoupled in Jurkat cells. We expect that our approach can be adapted to study other suspension cells.

Graphical Abstract

minxue@ucr.edu .

Conflicts of interest

There are no conflicts to declare.

[b]Electronic Supplementary Information (ESI) available: [details of any supplementary information available should be included here]. See DOI: 10.1039/x0xx00000x

Author Manuscript Author Manuscript Author Manuscript Author Manuscript

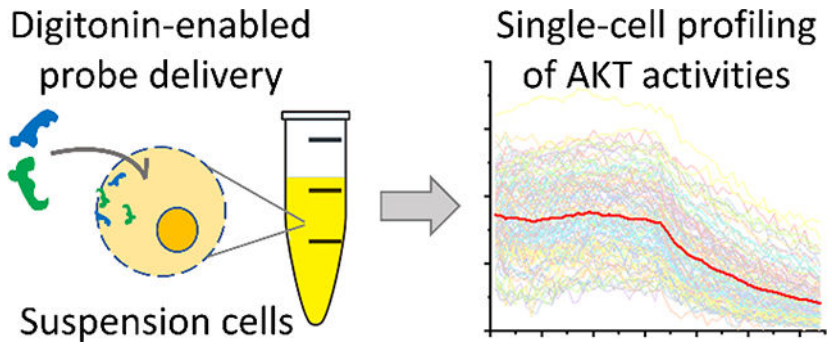

Digitonin allows the delivery of cyclic peptide-based imaging probes into suspension cells. This method enables time-resolved single-cell profiling of AKT signalling activities.

Introduction

Signalling proteins are critical governors of cellular activities. In many biological systems, the expression levels of signalling proteins are highly heterogeneous among the same group of cells. [1, 2] Understanding this heterogeneity through single-cell protein assays can help identify unique subpopulations and guide therapeutic decisions. [3, 4] For instance, cells with higher oncoprotein levels often represent a drug-resistant phenotype, and targeting these cells using combination chemotherapies can provide long-lasting effects. [5–8] However, despite the rapid development in the field of single-cell protein analysis, little is known about the heterogeneity in the time domain, i.e., the dynamical features of protein signalling.

Increasing evidence has demonstrated that the distinct temporal patterns of kinase signalling, such as oscillations, carry information that controls the cell's specific response and dictates cell fates.[9–11] Scrutinizing these dynamical behaviours of kinase signalling can help understand how various regulatory circuits shape signalling outputs.[11] Such a task is challenging since traditional immunolabeling-based analytical methods cannot be used inside living cells. Pioneering work on generically encoded reporting systems has enabled real-time readouts of kinase signalling activities. [12–16] However, there remain two critical challenges. First, these reporters focus on specific substrate sequences and subcellular locations. This design is perfect for delineating the signalling architecture but not well-suited for assessing the global status of signalling protein activities. Second, the expression of these reporters cannot be easily performed in delicate samples such as patient biopsies, which limits their translational applications.

To address these unmet needs, we have recently developed a chemical method to analyse single-cell kinase signalling dynamics, using cyclic peptide-based imaging probes that target specific kinase epitopes (Fig. 1a).[17] Compared with genetic approaches, [12, 13, 18, 19] our chemical probes provide a more direct readout of the signalling activity, which is not limited by a particular substrate type or influenced by the distribution of the kinase targets. In addition, these probes can be easily removed upon cell fixation, thereby permitting downstream single-cell analysis such as immunofluorescence-based protein quantification and enabling phenotype identifications.[17] Nevertheless, our original method

Author Manuscript Author Manuscript Author Manuscript Author Manuscript

required fusogenic liposomes to carry fluorescent probes into living cells, which can only be implemented in adherent cells. This requirement significantly limits the translational value of our original approach because of two reasons. First, blood samples are the most widely used and accessible clinical samples, which contain a rich repertoire of lymphoid and myeloid suspension cells.[20–22] Second, transforming clinical tumour samples into single-cell suspensions is straightforward and quick, but re-establishing them as adherent cells is a time-consuming and challenging process. Therefore, we need to improve our method, especially the probe delivery approach, to enable the analyses of suspension cells.

A popular technique for bringing small molecules into the intracellular space is to append a cell-penetrating tag.[23, 24] These tags include hydrophobic moieties that enable direct membrane penetration, as well as endocytosis-promoting groups such as poly-cationic residues and receptor substrate sequences such as RGD. Many examples have demonstrated the successful applications of these cell-penetrating tags; however, all those tags require chemical modifications to the molecular probes. Such a requirement could be detrimental to our intended applications, as our cyclic peptide probes are sensitive to modifications – complete loss of binding often occurs after simple structure alterations. In addition, the cytosolic delivery efficiency of these tags often varies significantly across different payloads. Considering that our cyclic peptide probes have different structures, we reasoned that cell-penetrating tags may not be an easily generalizable approach.

Another method for cytosolic delivery involves membrane perforation. Physical perforation strategies, such as magnetoporation,[25] sonoporation[26] and optoporation,[27] can enable the transportation of large molecules and have demonstrated their applications in gene delivery. However, those manipulations are time-consuming and they all require specialized instruments, which also limits their generalizability and suitability in our analytical scheme. On the other hand, chemical perforators such as saponins are known to induce transient pores on the cell membrane, where the degree of perforation is often tunable by varying the saponin concentration.[28, 29] These pores allow extracellular probe molecules to diffuse into the cytosol without any modifications to the probes. Encouraged by pioneering works on saponin-enabled peptide delivery, [30–32] we hypothesized that we could also use saponins to deliver the cyclic peptide probes into suspension cells.

Herein, we show that digitonin – a type of saponin – can indeed allow peptide probes to enter the cytosol of suspension cells (Fig. 1b). Using the cyclic peptide probes specific for detecting AKT activities, we demonstrate that this approach is applicable to different suspension cells, including adherent cells that are made into a single-cell suspension, myeloid cells, and lymphoid cells. We further show that this delivery approach is compatible with downstream immunofluorescence-based protein analysis by delineating the relationship between AKT expression level and the kinetic features of AKT signalling activities in THP-1 and Jurkat cells.

Author Manuscript Author Manuscript Author Manuscript Author Manuscript

Results and Discussion

Digitonin treatment on U87 cells

Digitonin is known to cause membrane perforation, which may lead to cell damage. Therefore, it is critical to optimize its concentration so that cells are not significantly harmed. We first evaluated the effect of digitonin on U87 cells, which were used extensively in our previous studies. Interestingly, we observed that 1 μg/mL digitonin treatment led to a slight increase in cell viability and metabolic activities, as evidenced by the elevated resazurin assay and MTT assay values (Fig. 2a, 2b). Raising the digitonin concentration to 3 μg/mL diminished the pro-growth effects and led to indistinguishable viability values as those from the control samples. Further increasing the digitonin concentration to 5 μg/mL caused inhibition of the cell viability, indicating significant toxicity to the cells. Because our goal is to continuously analyse AKT signalling activities in living cells, it is paramount not to substantially alter cell viability. Therefore, it was evident that 5 μg/mL was not acceptable for our purpose. Nevertheless, it is worth pointing out that 5 μg/mL was a commonly used digitonin concentration in the literature, especially those involving the delivery of large molecules. In those studies, the main goal was to perform the delivery instead of performing analysis.[30–32] Thus, the requirements are different here, and we must use lower digitonin concentrations to avoid cytotoxicity.

We then sought to check if digitonin treatment could indeed allow cyclic peptide probes to diffuse across the cell membrane. We treated the U87 single-cell suspension with varying concentrations of digitonin in the presence of our cyclic peptide probes, Rhodamine-cy(GSQTH) and Cy5-cy(YYTYT). After incubation and washing the cells, we loaded the cells into a microwell chip following established protocols and used a confocal microscope to evaluate the intracellular fluorescence signal. As shown in Fig. 2c, increasing digitonin concentrations led to elevating intracellular fluorescence intensities. This result is consistent with our expectation that higher digitonin concentrations would better facilitate the diffusion of cyclic peptide probes across the cell membrane. In addition, digitonin treatment did not alter the morphology of the cells (Supplementary Fig. S1). Taken together, 2 or 3 μg/mL turned out to be suitable digitonin concentrations for U87 cells.

Digitonin treatment on THP-1 cells

Since U87 cells are genuinely adherent cells, their properties are different from those true suspension cells such as myeloid and lymphoid cells. In order to test if digitonin would work on genuine suspension cells, we moved on to perform the experiments using THP-1 cells. These monocytic cells are of the myeloid lineage and are representative suspension cells.[33, 34] We first treated these THP-1 cells with varying concentrations of digitonin and evaluated the cell viability using the resazurin assay. As shown in Fig. 3a, all the tested digitonin concentrations led to lowered fluorescence signals compared with the control. This result indicated that THP-1 cells were more sensitive to digitonin treatment than U87 cells.

Nevertheless, because THP-1 cells may alter their metabolic pattern under external stimulation,[35, 36] the resazurin test result could not directly translate to cell viability. To better access cell viability, we resorted to cell counting. We treated THP-1 cells with

Author Manuscript Author Manuscript Author Manuscript Author Manuscript

different concentrations of digitonin and then incubated the cells for two days. We then counted the viable cells in each sample (Fig. 3b). Interestingly, we found that 1 μg/mL digitonin treatment promoted cell growth, and 2 μg/mL digitonin exhibited the same cell number as control. Higher digitonin concentrations (3 and 4 μg/mL) obviously inhibited cell proliferation, indicating that these concentrations caused substantial damage to the cells. This result was very similar to that from the U87 experiments but underscored that THP-1 cells were more prone to digitonin-induced metabolic alterations than U87 cells.

To evaluate if digitonin could also enable cyclic peptides to move across the THP-1 cell membrane, we co-treated these cells with digitonin and the peptide probes. We then loaded the cells onto the microwell chip, and performed confocal microscopy. We found that even 1 μg/mL of digitonin led to a substantial amount of cyclic peptide probes present in the cells (Fig. 3c). With increasing digitonin concentrations, the intracellular FRET signals also increased. This trend was consistent with our expectations and was similar to what we observed in the U87 experiments. Considering the cell viability results above (Fig. 3b), we reasoned that 2 μg/mL of digitonin was suitable for treating THP-1 cells.

THP-1 cells are sensitive to external stimuli and prone to differentiating into macrophage-like phenotypes (M1 and M2),[34] their cell morphology can serve as an additional parameter for evaluating the effects of digitonin treatment. Based on our observation (Supplementary Fig. S2), 1–4 μg/mL digitonin did not alter cell morphology, indicating that these concentrations did not cause phenotypical changes, which further validated the suitability of our approach.

Digitonin treatment on Jurkat cells

We then set to test if the digitonin approach was suitable for lymphoid cells, using Jurkat cells as a model system. Jurkat cells are immortalized human T lymphocytes, which are widely used in biomedical studies because of their close resemblance to normal T cells.[37] Similar to the THP-1 experiments, we first treated Jurkat cells with 1–4 μg/mL of digitonin and assessed its effect on cell viability using the resazurin assay. We found that digitonin treatment caused significantly lower metabolic activities, and this inhibition effect became more prominent with increasing digitonin concentrations (Fig. 4a). Because Jurkat cells were also sensitive to external perturbations and could alter their metabolic patterns in response to digitonin treatments,[38, 39] it was again necessary to validate our findings using cell counting. We treated the Jurkat cells with different concentrations of digitonin, incubated the cells for two days, and then counted the viable cells. Our results showed that cell proliferation was not inhibited by the digitonin treatment (Fig. 4b). Interestingly, we did not observe the pro-proliferation effects of 1 μg/mL digitonin treatment, like those in the U87 and THP-1 experiments. Based on these results, we concluded that 2 μg/mL of digitonin was suitable for treating Jurkat cells.

To assess the performance of the digitonin approach in delivering cyclic peptide probes into Jurkat cells, we incubated the cells in the presence of digitonin and the peptide probes and performed the confocal microscopy experiments as described above. We found that higher digitonin concentrations led to more intense FRET signals across the cell populations, which was consistent with the results from U87 and THP-1 experiments (Fig. 4c). We

Author Manuscript Author Manuscript Author Manuscript Author Manuscript

also observed substantial levels of FRET signals in samples treated with digitonin at low concentrations (1 and 2 μg/mL). In addition, no morphological changes were observed (Supplementary Fig. S3). Taken together, our results proved that digitonin treatment was an effective method for delivering cyclic peptide probes into Jurkat cells.

Single-cell profiling of AKT signalling activities in THP-1 cells

To further assess the performance of the digitonin approach, we delivered the cyclic peptide probes into THP-1 cells and performed continuous interrogation of the AKT signalling activities (Fig. 5a). Based on our results above, we chose 2 μg/mL as the optimal digitonin concentration. After incubating the cells with the peptide probes, we loaded the cells onto the microwell chip at a low concentration to achieve single-cell segregation. We then continuously monitored the FRET signals in those cells using confocal microscopy. During the imaging sessions, we added AZD8055 (an mTOR inhibitor) to the media to perturb the AKT signalling. At the end of the experiments, we fixed the cells in the microwells and performed immunofluorescence staining using an AKT antibody tagged with Alexa Fluor 647. The same cells were then imaged again to obtain the AKT immunofluorescence data.

The image stacks obtained from the live-cell imaging sessions contained the information of time-resolved AKT signalling activities at single-cell resolution. As shown in Fig. 5b, THP-1 cells exhibited fluctuating AKT activities before the drug addition, while the average signal levels among all the cells remained stable. This result was expected because the bulk-level AKT activity should not change significantly without external stimuli. Upon introducing the mTOR inhibitor (AZD8055), the average AKT activities gradually decreased. Since mTOR inhibition would cause de-phosphorylation of AKT at Ser473/474, the observed signal decrease was consistent with the mechanism of action. Notably, there was significant heterogeneity in the levels and rates of the signal decrease.

To better evaluate the cellular heterogeneity and to quantitatively compare the kinetic patterns of AKT signalling activities, we used the dynamic time warping (DTW) approach to analyse the time-resolved single-cell dataset. The DTW method was developed to evaluate the similarities in the time-evolution trends of signals without interference from speed variations. By performing pairwise DTW analysis,[41, 42] we converted the single-cell trajectories (Fig. 5b) into a distance matrix, where each matrix element represented the dissimilarities between a pair of single cells (Supplementary Fig. S4). Using this distance matrix, we were able to implement an agglomerative hierarchical clustering (AHC) strategy to identify subpopulations among the single cells. As shown in Fig. 5c, there were three distinct subpopulations (Supplementary Fig. S5, S6). As represented by the cluster centroids (Fig. 5d), each cluster displayed unique AKT signalling patterns. Cluster 1 cells exhibited strong fluctuations at basal condition, and relatively small responses to the drug perturbation. Cluster 2 cells and cluster 3 cells had similar drug responses, but cluster 2 cells displayed gradually decreasing AKT signalling activities at the basal condition, while cluster 3 cells had slightly increasing AKT activities before drug addition (Supplementary Fig. S6).

Because we were able to perform immunofluorescence staining on the same set of single cells, we could test if AKT expression levels varied among those three clusters. We extracted the AKT levels from all single cell and categorized them according to the cluster

Author Manuscript Author Manuscript Author Manuscript Author Manuscript

designations. We then used the Mann-Whitney test to compare the distributions among the three subpopulations. As shown in Fig. 5e, there were no statistically significant differences between clusters 2 and 3, while cluster 1 cells exhibited significantly lower AKT expression levels. This result suggested that AKT expression levels may affect the kinetic patterns of AKT signalling activities in THP-1 cells. In addition, lower AKT expression levels may link to more intense baseline fluctuations and less sensitivity to mTOR inhibition.

Single-cell profiling of AKT signalling activities in Jurkat cells

To test the generalizability of the digitonin approach, as well as the observed connection between AKT expression levels and AKT signalling patterns, we performed similar experiments using Jurkat cells. As shown in Fig. 6a, at basal condition, Jurkat cells exhibited much higher heterogeneity in AKT signalling activity levels compared with THP-1 cells. This result was expected because Jurkat cells were known to be highly heterogeneous.[40] Upon mTOR inhibition, the AKT signalling levels decreased gradually. On average, the signal decreased by 40% in 10 min, consistent with the results from THP-1 cells. Interestingly, some cells exhibited transient signal increase immediately after the mTOR inhibitor addition. Using pairwise DTW and AHC analysis, we identified three subpopulations among the Jurkat cells (Fig. 6b, Supplementary Fig. S7, S8). Notably, each clusters had unique features (Fig. 6c, Supplementary Fig. S9). Cluster 1 cells displayed quick dips immediately after drug addition, followed by prounounced signal decrease over the time course. Cluster 2 cells showed slight jumps immediately after the drug addition, followed by prominant signal decrease. Cluster 3 cells exhibited much stronger jumps after drug addition, and their overall signal decrease over the time course were much smaller compared with the other two clusters. Surprisingly, the AKT expression levels did not vary significantly across these three clusters. This result indicated that the kinetic patterns of AKT signalling decoupled from the AKT expression levels in Jurkat cells.

Experimental

Chemicals and reagents

Mannitol, HEPES, potassium chloride (KCl), sodium succinate, ethylene glycol-bis(β-aminoethyl ether)-N,N,N′,N′-tetraacetic acid (EGTA), ethylenediaminetetraacetic acid (EDTA), bovine serum albumin (BSA), resazurin, (3-(4,5-dimethylthiazol-2-yl)-2,5-diphenyltetrazolium bromide (MTT), and digitonin were purchased from Sigma-Aldrich (St. Louis, MO). Phosphate-buffered saline (PBS), Dulbecco's Modified Eagle Medium (DMEM), RPMI media, penicillin-streptomycin (pen-strep), and heat-inactivated fetal bovine serum (FBS) were purchased from Thermo Fisher Scientific (Waltham, MA).

Cell culture

All cells were purchased from ATCC (the American Type Culture Collection). U87 cells were cultured in DMEM with 10% FBS and 100 U/mL of pen-strep. THP-1 cells and Jurkat cells were cultured in RPMI-1640 with 10% FBS and 100 U/mL of pen-strep. All cell cultures were maintained in a humidified 5% CO_2 (v/v) incubator at 37 °C.

Author Manuscript Author Manuscript Author Manuscript Author Manuscript

Digitonin treatment

Cells were washed three times in mannitol experiment buffer (MEB) before digitonin treatment. The washed cells were resuspended in MEB buffer and incubated with digitonin (various concentrations) for 20 minutes, with or without the presence of the peptide probes. Afterwards, the cells were washed three times with fresh culture media to ensure the removal of digitonin.

Cell viability tests

Resazurin assay.—Cells treated with different concentrations of digitonin were seeded in a 96-well plate and incubated for 5 hours. 40 μL of 0.06 mg/mL resazurin PBS solution was then added into each well, followed by incubation at 37 °C for 3 hours. The resulted fluorescence signals were recorded by a plate reader (560 nm excitation, 590 nm emission).

MTT assay.—U87 cells treated with different concentrations of digitonin were seeded in the 96-well plate and incubated overnight. 10 μL of 12 mM MTT/PBS solution was added to each well and the plate was incubated at 37 °C for 4 hours. The absorbance values at 570 nm were recorded using a plate reader.

Cell number counting.—Cells were seeded in a 96-well plate, and different concentrations of digitonin were added. The cell numbers were counted using a hemocytometer after a 2-day incubation.

Confocal imaging

Evaluating digitonin treatment results.—Cells were loaded with the AKT cyclic peptide probes (RhoB-GSQTH, 2 μM in MEB; Cy5-YYTYT, 50 μM in MEB) using the digitonin treatment approach described above. Cells were then loaded on the microwell chip and imaged using a confocal microscope (Zeiss 880) following established protocols.

Single-cell monitoring of AKT signalling activities.—THP-1 cells and Jurkat cells were loaded onto the microwell chip at a concentration of 800 k/mL and incubated at 37 °C. Extra cells were scraped off the chip surface, and the chip was washed with fresh cell culture media. The cells were imaged using a confocal microscope (Zeiss 880) following established protocols. AZD8055 was introduced to reach final concentrations of 1 μM (THP-1) and 0.5 μM (Jurkat) during the experiments.

Immunofluorescence

The cells were fixed with cold methanol (−20 °C) on the chip right after the confocal imaging. Five minutes later, the chip was washed with PBS (5 minutes X 3 times). After fixation, the chip loaded with cells was blocked by goat serum at room temperature for an hour. The AKT detection antibody solution was prepared by mixing 2.5 μL of AKT antibody solution (as purchased, Cell Signalling Technology #5186) and 1 mL of 1% BSA in PBS. The cells were incubated with the detection antibody solution on the chip at 4 °C overnight. After incubation, the chip was washed with PBS and then imaged using the confocal microscope (Zeiss 880).

Author Manuscript Author Manuscript Author Manuscript Author Manuscript

Single-cell data analysis

Data extraction.—The obtained single-cell image stacks were analysed using Fiji following established protocols. The FRET signal intensities from every single cell were plotted to generate single-cell AKT signalling trajectories. The AKT expression levels were obtained from extracting the fluorescence intensities from each single cell after the immunostaining.

DTW analysis.—Pairwise dynamic time warping analysis was performed using the *dtw* function in MATLAB®. The result was presented as a distance matrix, where each matrix element represented the dissimilarity between two single-cell trajectories.

AHC analysis.—The clustering was performed with the *Hierarchical Cluster Analysis* tool in OriginPro®2019b. The clusters were identified based on the Euclidean distances between elements and Ward's method. The result was a dendrogram showing different clusters in the dataset. This dendrogram was then combined with the heatmap generated from the DTW analysis to highlight the clusters.

Mann-Whitney tests.—The AKT expression level distributions from the three clusters were evaluated using Mann-Whitney tests. This analysis was performed in OriginPro®2019b.

Conclusions

In conclusion, we have established a method for delivering cyclic peptide-based imaging probes into suspension cells using digitonin. At low concentrations (1–2 μg/mL), digitonin was not toxic to the cells but was able to transiently permeabilize the plasma membrane, which allowed the diffusion of peptide probes into the cytosol. We showed that this digitonin strategy was applicable to various cell types, such as single-cell suspension of genuinely adherent cells (U87), myeloid cells (THP-1), and lymphoid cells (Jurkat).

Using the digitonin delivery method, we further demonstrated the analysis of AKT signalling activities in THP-1 and Jurkat cells, followed by the immunofluorescence quantitation of AKT expression levels. With these datasets, we showed that under mTOR inhibition, the kinetic features of AKT signalling activities and the AKT expression levels were related in THP-1 cells, but are decoupled in Jurkat cells. Our results showcased the application of our strategy, underscored the AKT signalling heterogeneity in different cell lines, and highlighted how such an analytical workflow led to a better understanding of the single-cell AKT signalling dynamics.

Supplementary Material

Refer to Web version on PubMed Central for supplementary material.

Acknowledgements

We gratefully acknowledge the financial support from grant 5R21EB025393 from the US National Institutes of Health.

Author Manuscript Author Manuscript Author Manuscript Author Manuscript

References

1. Lim JS, Ibaseta A, Fischer MM, Cancilla B, O'Young G, Cristea S, Luca VC, Yang D, Jahchan NS, Hamard C, Antoine M, Wislez M, Kong C, Cain J, Liu YW, Kapoun AM, Garcia KC, Hoey T, Murriel CL and Sage J, Nature, 2017, 545, 360–364. [PubMed: 28489825]
2. Welch DR, Cancer Research, 2016, 76, 4. [PubMed: 26729788]
3. Wei W, Shin YS, Xue M, Matsutani T, Masui K, Yang H, Ikegami S, Gu Y, Herrmann K, Johnson D, Ding X, Hwang K, Kim J, Zhou J, Su Y, Li X, Bonetti B, Chopra R, James CD, Cavenee WK, Cloughesy TF, Mischel PS, Heath JR and Gini B, Cancer Cell, 2016, 29, 563–573. [PubMed: 27070703]
4. Xue M, Wei W, Su Y, Kim J, Shin YS, Mai WX, Nathanson DA and Heath JR, Journal of the American Chemical Society, 2015, 137, 4066–4069. [PubMed: 25789560]
5. Pisco AO and Huang S, British Journal Of Cancer, 2015, 112, 1725. [PubMed: 25965164]
6. Pisco AO, Brock A, Zhou J, Moor A, Mojtahedi M, Jackson D and Huang S, Nature communications, 2013, 4, 2467.
7. Su Y, Wei W, Robert L, Xue M, Tsoi J, Garcia-Diaz A, Homet Moreno B, Kim J, Ng RH, Lee JW, Koya RC, Comin-Anduix B, Graeber TG, Ribas A and Heath JR, Proceedings of the National Academy of Sciences, 2017, 114, 13679.
8. Shaffer SM, Dunagin MC, Torborg SR, Torre EA, Emert B, Krepler C, Beqiri M, Sproesser K, Brafford PA, Xiao M, Eggan E, Anastopoulos IN, Vargas-Garcia CA, Singh A, Nathanson KL, Herlyn M and Raj A, Nature, 2017, 546, 431. [PubMed: 28607484]
9. Andrews SS, Peria WJ, Yu RC, Colman-Lerner A and Brent R, Cell Systems, 2016, 3, 444–455.e442. [PubMed: 27894998]
10. Artyomov MN, Das J, Kardar M and Chakraborty AK, Proceedings of the National Academy of Sciences, 2007, 104, 18958.
11. Santos SDM, Verveer PJ and Bastiaens PIH, Nature Cell Biology, 2007, 9, 324. [PubMed: 17310240]
12. Ting AY, Kain KH, Klemke RL and Tsien RY, Proceedings of the National Academy of Sciences, 2001, 98, 15003.
13. Oldach L and Zhang J, Cell Chem. Biol, 2014, 21, 186–197.
14. Sasaki K, Sato M and Umezawa Y, Journal of Biological Chemistry, 2003, 278, 30945–30951.
15. Kunkel MT, Ni Q, Tsien RY, Zhang J and Newton AC, The Journal of biological chemistry, 2005, 280, 5581–5587. [PubMed: 15583002]
16. Gao X and Zhang J, Molecular biology of the cell, 2008, 19, 4366–4373. [PubMed: 18701703]
17. Shao S, Li Z, Cheng H, Wang S, Perkins NG, Sarkar P, Wei W and Xue M, Journal of the American Chemical Society, 2018, 140, 13586–13589. [PubMed: 30351133]
18. Gross SM and Rotwein P, Journal of cell science, 2015, 128, 2509–2519. [PubMed: 26040286]
19. Gao X and Zhang J, Communicative & integrative biology, 2009, 2, 32–34. [PubMed: 19704863]
20. Heath JR, Ribas A and Mischel PS, Nature Reviews Drug Discovery, 2016, 15, 204–216. [PubMed: 26669673]
21. Ignatiadis M, Sledge GW and Jeffrey SS, Nature Reviews Clinical Oncology, 2021, 18, 297–312.
22. Schafflick D, Xu CA, Hartlehnert M, Cole M, Schulte-Mecklenbeck A, Lautwein T, Wolbert J, Heming M, Meuth SG, Kuhlmann T, Gross CC, Wiendl H, Yosef N and Meyer zu Horste G, Nature Communications, 2020, 11, 247.
23. Qian Z, Martyna A, Hard RL, Wang J, Appiah-Kubi G, Coss C, Phelps MA, Rossman JS and Pei D, Biochemistry, 2016, 55, 2601–2612. [PubMed: 27089101]
24. Guidotti G, Brambilla L and Rossi D, Trends in Pharmacological Sciences, 2017, 38, 406–424. [PubMed: 28209404]
25. Liu D, Wang L, Wang Z and Cuschieri A, Nano Letters, 2012, 12, 5117–5121. [PubMed: 22950948]
26. Helfield B, Chen X, Watkins SC and Villanueva FS, Proceedings of the National Academy of Sciences, 2016, 113, 9983.

Author Manuscript Author Manuscript Author Manuscript Author Manuscript

27. Patskovsky S, Qi M and Meunier M, Analyst, 2020, 145, 523–529. [PubMed: 31761924]
28. Korchowiec B, Gorczyca M, Wojszko K, Janikowska M, Henry M and Rogalska E, Biochimica et Biophysica Acta (BBA) - Biomembranes, 2015, 1848, 1963–1973. [PubMed: 26055895]
29. Lorent JH, Quetin-Leclercq J and Mingeot-Leclercq M-P, Organic & Biomolecular Chemistry, 2014, 12, 8803–8822. [PubMed: 25295776]
30. Deng J, Carlson N, Takeyama K, Dal Cin P, Shipp M and Letai A, Cancer Cell, 2007, 12, 171–185. [PubMed: 17692808]
31. Mai WX, Gosa L, Daniels VW, Ta L, Tsang JE, Higgins B, Gilmore WB, Bayley NA, Harati MD, Lee JT, Yong WH, Kornblum HI, Bensinger SJ, Mischel PS, Rao PN, Clark PM, Cloughesy TF, Letai A and Nathanson DA, Nature medicine, 2017, 23, 1342–1351.
32. Ryan J and Letai A, Methods (San Diego, Calif.), 2013, 61, 156–164.
33. Bosshart H and Heinzelmann M, Ann Transl Med, 2016, 4, 438–438. [PubMed: 27942529]
34. Genin M, Clement F, Fattaccioli A, Raes M and Michiels C, BMC Cancer, 2015, 15, 577. [PubMed: 26253167]
35. Mussotter F, Potratz S, Budczies J, Luch A and Haase A, Toxicology and Applied Pharmacology, 2018, 340, 21–29. [PubMed: 29289672]
36. Abuawad A, Mbadugha C, Ghaemmaghami AM and Kim D-H, Metabolomics, 2020, 16, 33. [PubMed: 32114632]
37. Abraham RT and Weiss A, Nature Reviews Immunology, 2004, 4, 301–308.
38. Fernández-Ramos AA, Marchetti-Laurent C, Poindessous V, Antonio S, Petitgas C, Ceballos-Picot I, Laurent-Puig P, Bortoli S, Loriot M-A and Pallet N, Scientific Reports, 2017, 7, 10550. [PubMed: 28874730]
39. Liao W, Tan G, Zhu Z, Chen Q, Lou Z, Dong X, Zhang W, Pan W and Chai Y, Journal of Proteome Research, 2012, 11, 5109–5123. [PubMed: 23025307]
40. Snow K and Judd W, Experimental Cell Research, 1987, 171, 389–403. [PubMed: 3476309]
41. Myers CS and Rabiner LR, Bell System Technical Journal, 1981, 60, 1389–1409.
42. Vaughan N and Gabrys B, Procedia Computer Science, 2016, 96, 465–474.

Author Manuscript Author Manuscript Author Manuscript Author Manuscript

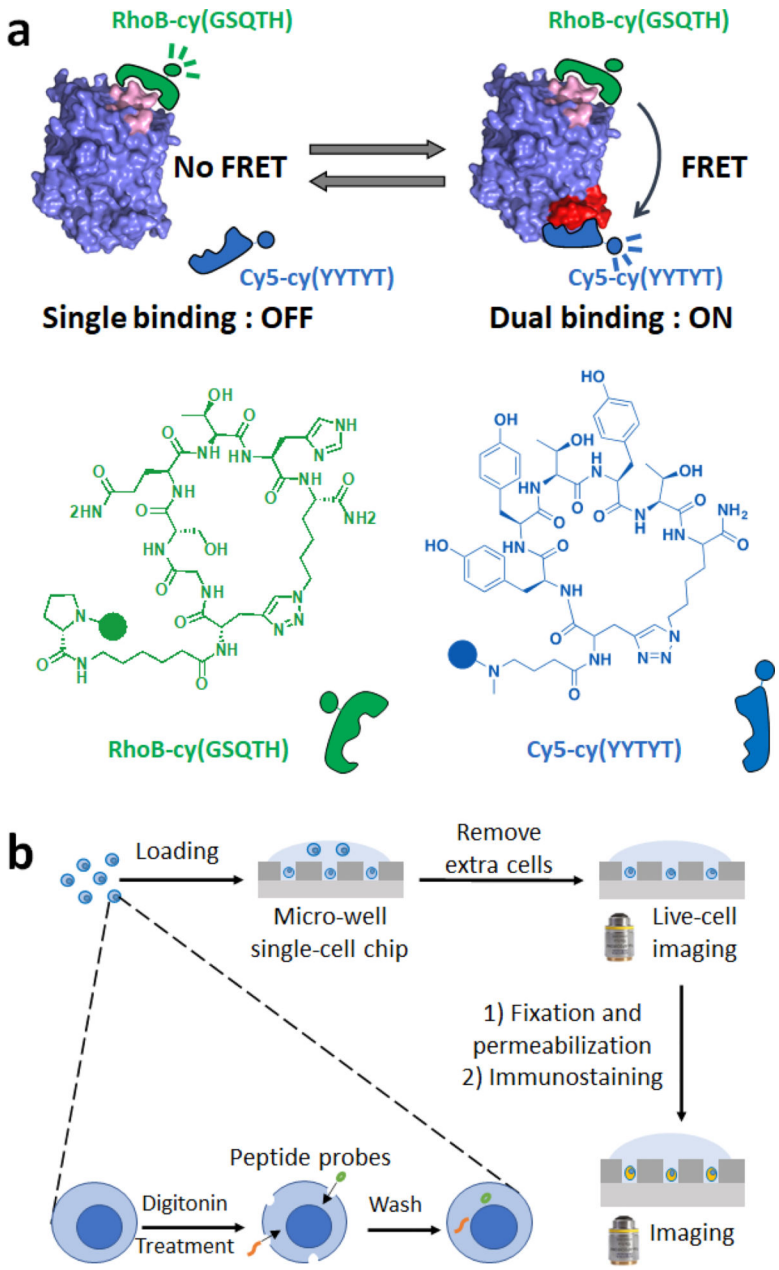

Fig. 1.

a) The mechanism of interrogating AKT signalling activities using a pair of cyclic peptide probes. **b)** Digitonin can transiently permeabilize the cells and allow the peptide probes to diffuse into the cells. The cells can then be loaded onto a single-cell microwell chip for AKT signalling analysis.

Author Manuscript Author Manuscript Author Manuscript Author Manuscript

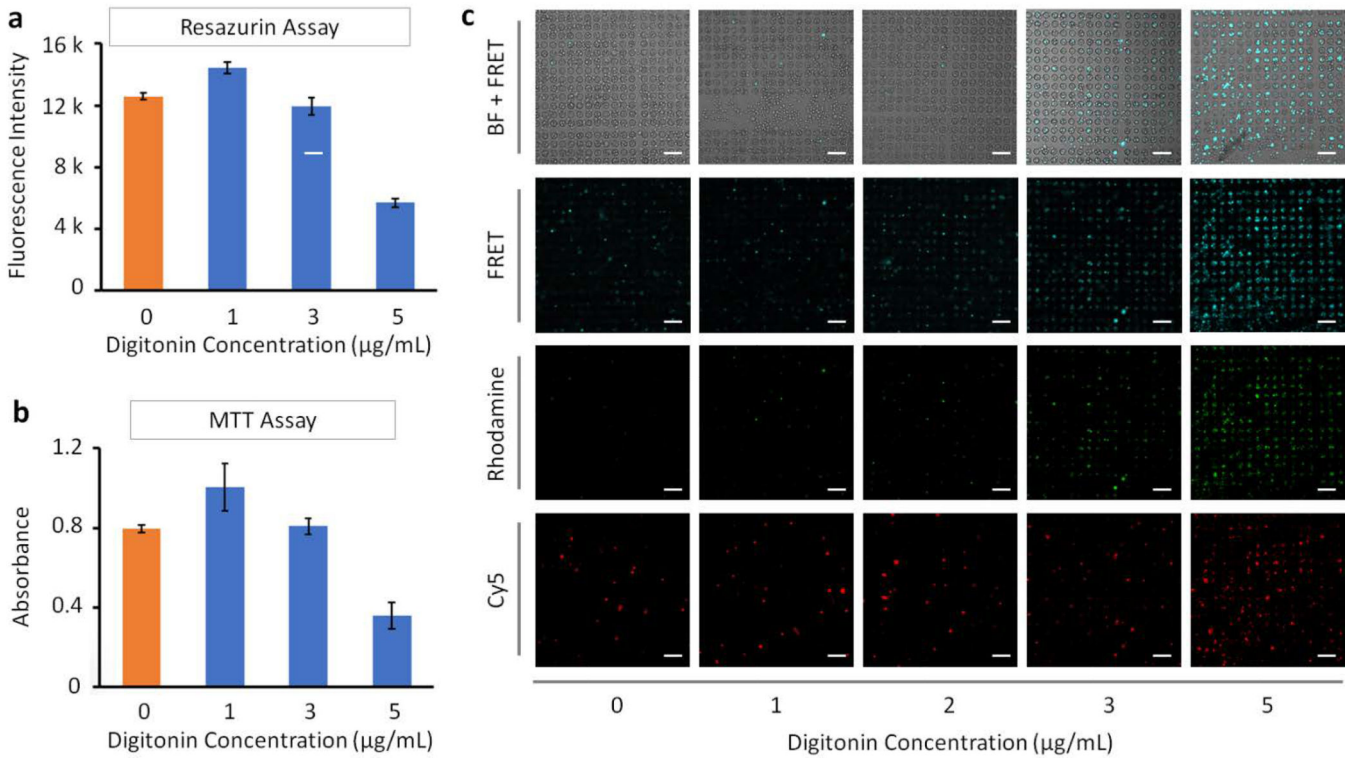

Fig. 2.

The effect of digitonin treatment on U87 cells. **a)** Resazurin assay and **b)** MTT assay results were used to evaluate cell viability. **c)** Confocal images of U87 cells treated with different concentrations of digitonin and loaded with the peptide probes. Cells were placed on a microwell chip to facilitate the imaging. Scale bars: 100 μm. Microwell chips with different well diameters were used for the samples.

Author Manuscript Author Manuscript Author Manuscript Author Manuscript

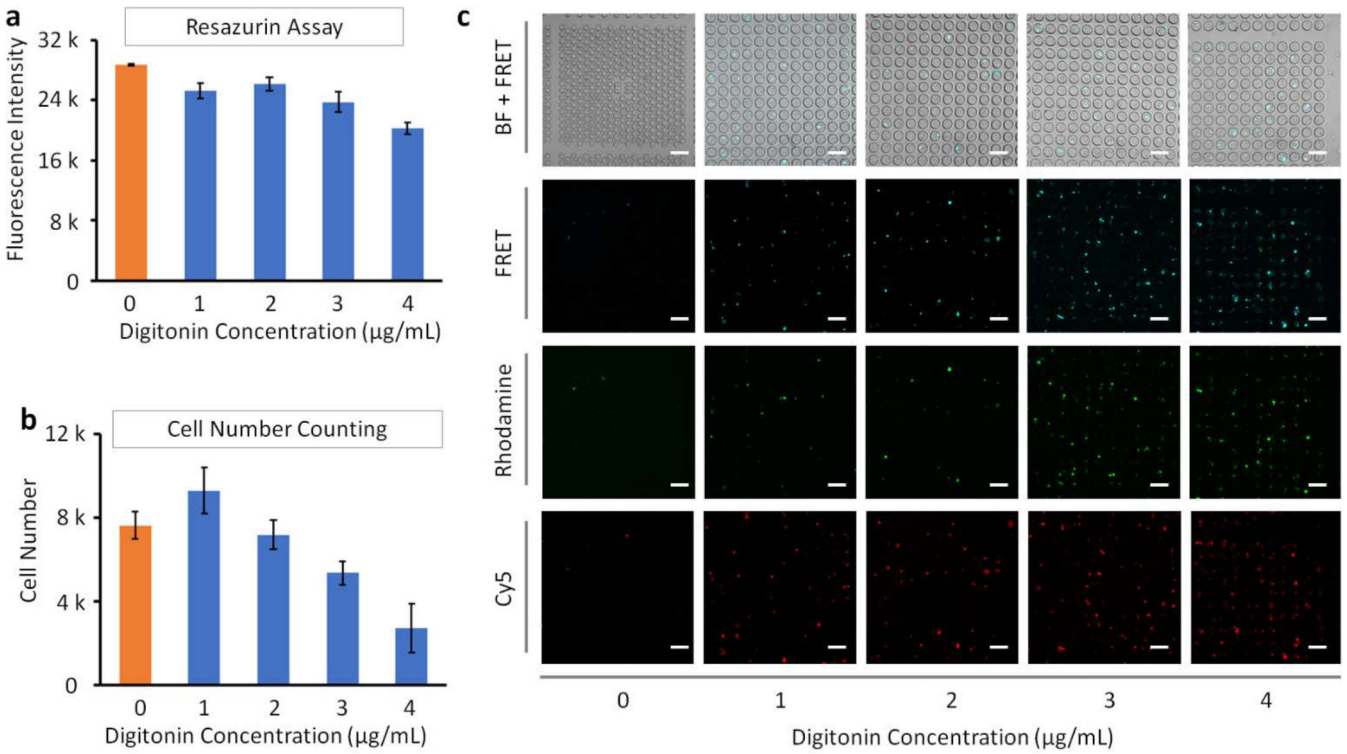

Fig. 3.

The effect of digitonin treatment on THP-1 cells. **a)** Resazurin assay and **b)** cell counting assay results were used to evaluate cell viability. **c)** Confocal images of THP-1 cells treated with digitonin and loaded with the peptide probes. Cells were placed on a microwell chip to facilitate the imaging. Scale bars: 100 μm. Microwell chips with different well diameters were used for the samples.

Author Manuscript Author Manuscript Author Manuscript Author Manuscript

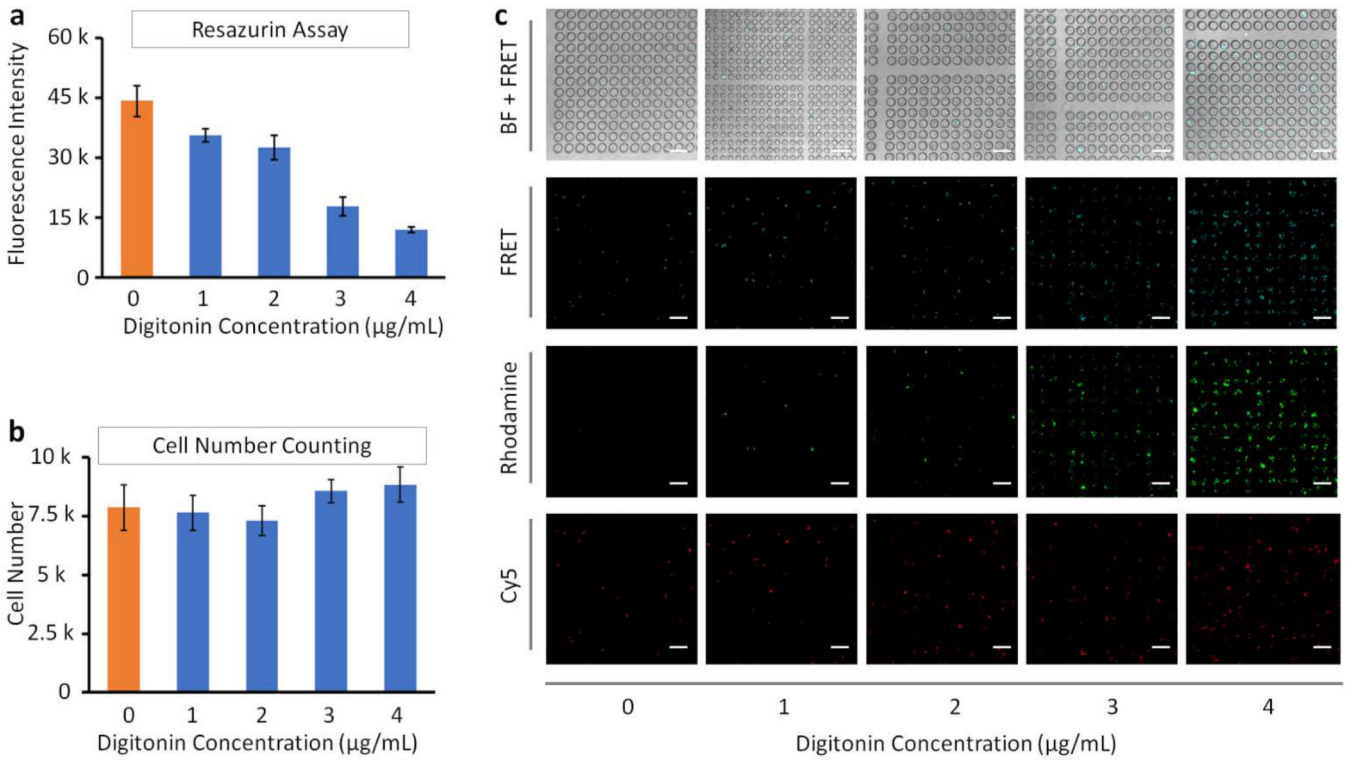

Fig. 4.

The effect of digitonin treatment on Jurkat cells. **a)** Resazurin assay and **b)** cell counting assay results were used to evaluate cell viability. **c)** Confocal images of Jurkat cells treated with digitonin and loaded with the peptide probes. Cells were placed on a microwell chip to facilitate the imaging. Scale bars: 100 μm. Microwell chips with different well diameters were used for the samples.

Author Manuscript Author Manuscript Author Manuscript Author Manuscript

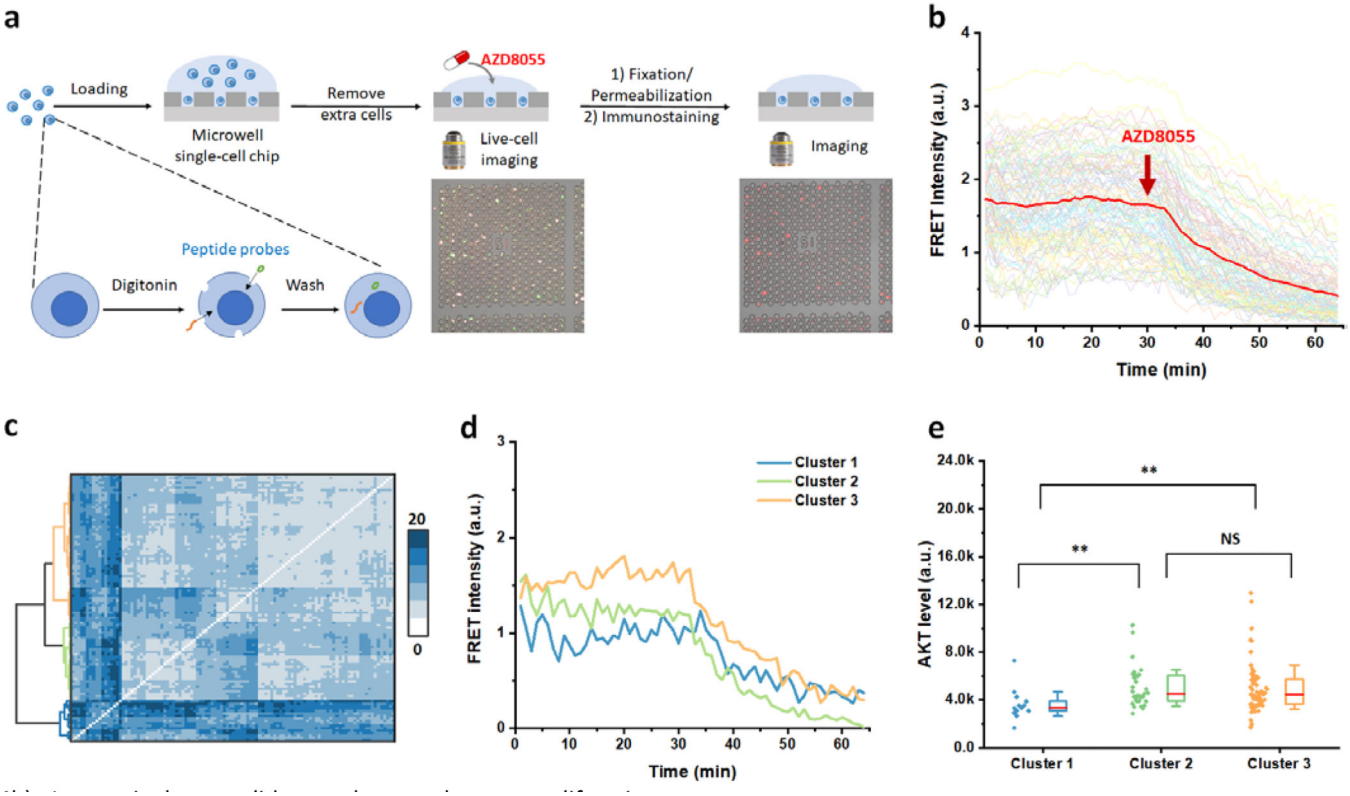

Fig. 5.

a) Schematic illustration of the experiment process. THP-1 cells were first treated with digitonin to allow peptide probes to diffuse into the cytosol. After washing and sealing the cells, the probe-loaded cells were placed on a microwell single-cell chip, where cells sank to the bottom of the wells. Continuous live-cell confocal imaging allowed monitoring AKT signalling activities from the single cells, and subsequent immunofluorescence staining enabled quantitation of AKT expression levels from the same set of single cells. **b)** The single-cell AKT signalling trajectories generated by extracting signal intensities from the time-resolved image stacks. Each thin trace represents a single cell. The bold red trace represents the average activities from all the monitored single cells. **c)** Agglomerative hierarchical clustering results generated from the dynamic time warping distance (DTW) matrix. Three distinct clusters were identified. The intensity of each pixel represents the corresponding DTW distance between two single cells. **d)** AKT signalling patterns of the cluster centroids. **e)** AKT expression levels obtained from the immunofluorescence staining results. The red horizontal lines represent the median levels in each cluster. The boxes denote the middle two quartiles, and the whiskers represent the standard deviation of each distribution. Mann-Whitney tests were used to compare the distributions. **: $p < 0.01$. NS: not significant.

Author Manuscript Author Manuscript Author Manuscript Author Manuscript

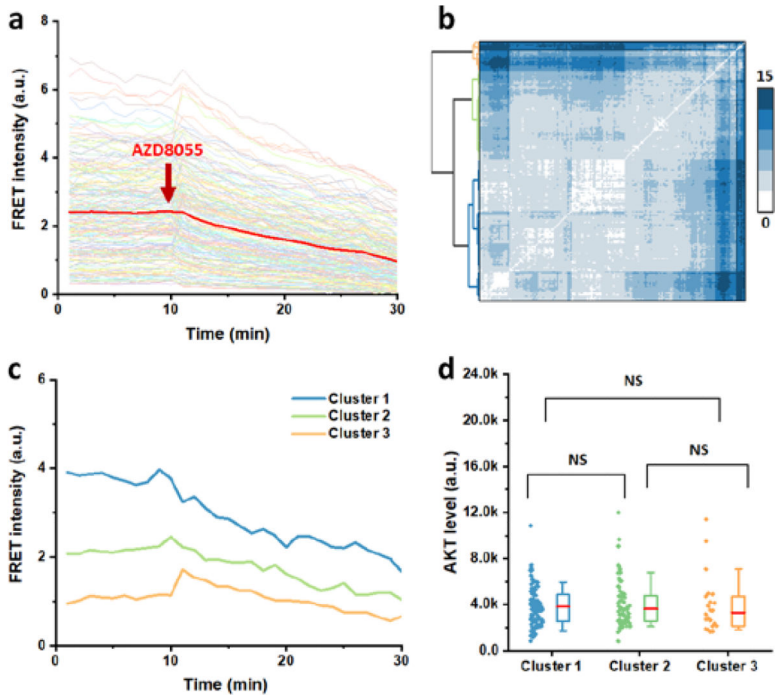

Fig. 6.

Single-cell profiling of AKT signalling activities in Jurkat cells **a)** The single-cell AKT signalling trajectories of Jurkat cells. Each thin trace represents a single cell. The bold red trace represents the average activities from all the monitored single cells. **c)** Agglomerative hierarchical clustering results generated from the DTW matrix. Three distinct clusters were identified. The intensity of each pixel represents the corresponding DTW distance between two single cells. **d)** AKT signalling patterns of the cluster centroids. **e)** AKT expression levels obtained from the immunofluorescence staining results. The red horizontal lines represent the median levels in each cluster. The boxes denote the middle two quartiles, and the whiskers represent the standard deviation of each distribution. Mann-Whitney tests were used to compare the distributions. NS: not significant.